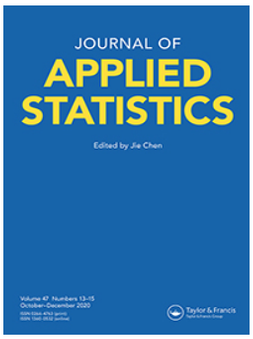

Journal of Applied Statistics

ISSN: (Print) (Online) Journal homepage: www.tandfonline.com/journals/cjas20

Models induced from critical birth–death process with random initial conditions

A. Tchorbadjieff & P. Mayster

To cite this article: A. Tchorbadjieff & P. Mayster (2020) Models induced from critical birth–death process with random initial conditions, Journal of Applied Statistics, 47:13-15, 2862-2878, DOI: 10.1080/02664763.2020.1732309

To link to this article: https://doi.org/10.1080/02664763.2020.1732309

JOURNAL OF APPLIED STATISTICS
2020, VOL. 47, NOS. 13–15, 2862–2878
https://doi.org/10.1080/02664763.2020.1732309

Taylor & Francis
Taylor & Francis Group

REVIEW ARTICLE

Models induced from critical birth–death process with random initial conditions

A. Tchorbadjieff and P. Mayster

Institute of Mathematics and Informatics, Bulgarian Academy of Science, Sofia, Bulgaria

ABSTRACT

In this work, we study a linear birth–death process starting from random initial conditions. First, we consider these initial conditions as a random number of particles following different standard probabilistic distributions – Negative-Binomial and its closest Geometric, Poisson or Pólya–Aeppli distributions. It is proved analytically and numerically that in these cases the random number of particles alive at any positive time follows the same probability law like the initial condition, but with different parameters depending on time. The random initial conditions cannot change the critical parameter of branching mechanism, but they impact the extinction probability. Finally, the numerical model is extended to an application for studying branching processes with more complex initial conditions. This is demonstrated with a linear birth–death process initialised with Pólya urn sampling scheme. The obtained preliminary results for particle distribution show close relation to Pólya–Aeppli distribution.

ARTICLE HISTORY
Received 19 October 2018
Accepted 15 February 2020

KEYWORDS
Branching processes; linear birth–death process; Negative-Binomial distribution; Pólya–Aeppli distribution; stochastic simulations; Pólya urn; initial condition

AMS SUBJECT CLASSIFICATIONS
60J80; 60K05

1. Introduction

When G. U. Yule tried to give quantitative measure for evolution theory's connection between the size of the population and the area which is occupied, he introduced the basic discrete birth process with constant rate [30]. Soon, Furry modelled nuclear chain reactions as an extension of the classical Yule process, assuming that the particles could double with time-dependent rate in any specific medium. Then, the theory has been expanded with many different modified implementations of the classical Yule–Furry processes. They have been developed with the aim to model processes in different fields – from demography and population biology to server queueing modelling [10]. Recently, a very interesting relation between Yule and Poisson processes appeared in [9]. Many of them follow the most prominent works in the field of branching processes, mainly summarized in Feller's contributions to mathematical biology [5] and in the review of the history of branching processes by David G. Kendal in [14].

The physics is a very promising field for the implementation of branching processes, especially for modelling of nuclear chain reactions and electromagnetic cascades. This had

CONTACT A. Tchorbadjieff atchorbadjieff@math.bas.bg Institute of Mathematics and Informatics, Bulgarian Academy of Science, Sofia, Bulgaria

been noticed very early and resulted in the first detailed mathematical description of these branching processes in the famous Theodore Harris' book [12]. However, the straightforward computation and implementation of available analytical results are not possible due to the complicated nature of the studied processes, most clearly demonstrated in the cosmic ray physics. As a result, the computational modelling remained as the only possible solution for studying similar complex branching processes since their early ages [16]. Soon, with the rapid growth of computational power, the number of different Monte Carlo applications grew and now they cover a very wide range of different topics. For instance, the most important contemporary tools with a strictly specific focus on particle detectors and fundamental particle physics are GEANT4 [1], FLUKA [6] and CORSIKA [13].

Usually, the well-developed numerical applications are mainly used to model a particular topic or process following predefined assumptions. Many of them rely on model-dependent initial conditions that vary model input parameters to adjust the observable outcome. This narrows the results to the studied topic without options to be used in different fields. A possible solution to obtain more generalized results for branching processes is to estimate the probability density functions with repeated numerical experiments. The best way to implement similar step tracking iterative methods is the implementation of Monte Carlo Markov chains (MCMC), similar to [23,25]. Initially, these tools must be implemented and verified on a special class of models. Then, the working numerical experiment can be modified with changes in the initial conditions or parameters of branching. Finally, the methods of statistical inference could be used for the estimation of probability distribution [see 24]. Using this solution model, in this work, we created a numerical method for studying the development of branching birth–death process initiated by a random number of particles from different initial conditions.

To describe the initial conditions we consider the most important discrete distributions – Negative-Binomial and its closest Geometric, Poisson or Pólya–Aeppli distributions [17,18]. The selection of these distributions is due to their importance not only in probability theory but also in a wide range of available applications, such as [2,21,25]. The obtained results are independently confirmed with analytical and numerical solutions only for the case of a critical branching process. Finally, in the last chapter, the experiment is modified with the selection of Pólya urn sampling scheme as a generator of the initial condition. The estimates of resulting distributions are determined numerically as a demonstration of possibilities of numerical experiments.

2. Model selection

The branching processes describe systems of 'particles' with the phenomena of multiplication. The principal assumption is the independence of particle evolution without interaction. This model is completely characterised by the offspring number of particles and their lifetime. Both, the Yule and linear birth–death processes, are special cases of Markov branching processes. Following the classical theory, the branching mechanism of reproduction for the linear birth–death (B–D) process is defined by the quadratic function $h(s) = ps^2 + 1 - p,\ 0 < p \leq 1,\ |s| \leq 1$, and exponentially distributed lifetime of particles with parameter $K > 0$ [see 4,20]. The infinitesimal generating function is given by

$$f(s) := K(h(s) - s) = K(ps^2 - s + 1 - p), \quad 0 < p \leq 1,\ |s| \leq 1. \tag{1}$$

The exponential lifetime of particles gives the Markov property of the process $X(t), t \geq 0, X(0) = 1$, describing the number of particles alive at the time $t > 0$. The probability generating function (p.g.f.) of $X(t)$ is defined by

$$F(t,s) = \sum_{k=0}^{\infty} s^k P(X(t) = k \,|\, X(0) = 1) \tag{2}$$

and satisfies respectively the non-linear backward and linear forward Chapman–Kolmogorov equations:

$$\frac{\partial}{\partial t}\left(F(t,s)\right) = f\left(F(t,s)\right), \tag{3}$$

$$\frac{\partial}{\partial t}\left(F(t,s)\right) = f(s)\frac{\partial}{\partial s}\left(\left(F(t,s)\right), \right. \tag{4}$$

with the initial condition $F(0,s) = s$.

In accordance with Equations (1) and (2), the mean of the infinitesimal offsprings number is denoted with $m = (\mathrm{d}f/\mathrm{d}s)(1) = K(2p-1)$, and expected value of the number of particles alive at time $t > 0$ is equal to $E[(X(t)] = e^{mt}, t > 0$. This exponential rate is exactly the distinctive trait (feature) of branching processes.

Every branching process $X(t)$ is classified as either supercritical, critical or subcritical by the inequalities for mean, i.e. respectively $m > 0$, $m = 0$, $m < 0$. This classification is in accordance with the notion of the ultimate extinction probability, denoted by

$$q = \lim_{t\to\infty} P(X(t) = 0) = \lim_{t\to\infty} F(t,0) \geq 0,$$

and given by the smallest solution of the equation $h(s) = s$ in the interval $[0,1]$. For the extinction probability is valid that $q = 1$ if and only if $m \leq 0$ [see 20]. Respectively, for supercritical process $m > 0$ and $0 \leq q < 1$. The differences are demonstrated graphically in Figure 1.

In this work, the critical case is only considered. Thus the studied process is defined by its p.g.f. $F(t,s)$ representing the solution of the Equations (3) and (4), as follows:

$$F(t,s) = 1 - \frac{2(1-s)}{2 + Kt(1-s)}, \quad m = 0,\ p = 1/2,\ q = 1. \tag{5}$$

Let us denote the extinction probability by the time $t > 0$ with $A(t) = F(t,0)$. Then the p.g.f. (5) of the critical linear B–D process $X(t)$ can be presented as

$$F(t,s) = A(t) + [1 - A(t)]\left(\frac{[1-\alpha(t)]s}{1-\alpha(t)s}\right), \quad A(t) = \alpha(t) = \frac{Kt}{2+Kt}. \tag{6}$$

This representation signifies by itself that for any fixed $t > 0$ the random variable $X(t)$ follows the zero-modified geometric distribution, with parameters $A = A(t)$ and $\alpha = \alpha(t)$, where

$$P(X(t) = 0) = A, \quad P(X(t) = k) = (1-A)(1-\alpha)\alpha^{k-1},\ k = 1,2,\ldots.$$

The obtained expressions for $A(t)$ and $\alpha(t)$ for subcritical, critical and supercritical processes, i.e. $m < 0, m = 0, m > 0$, are summarized in Table 1.

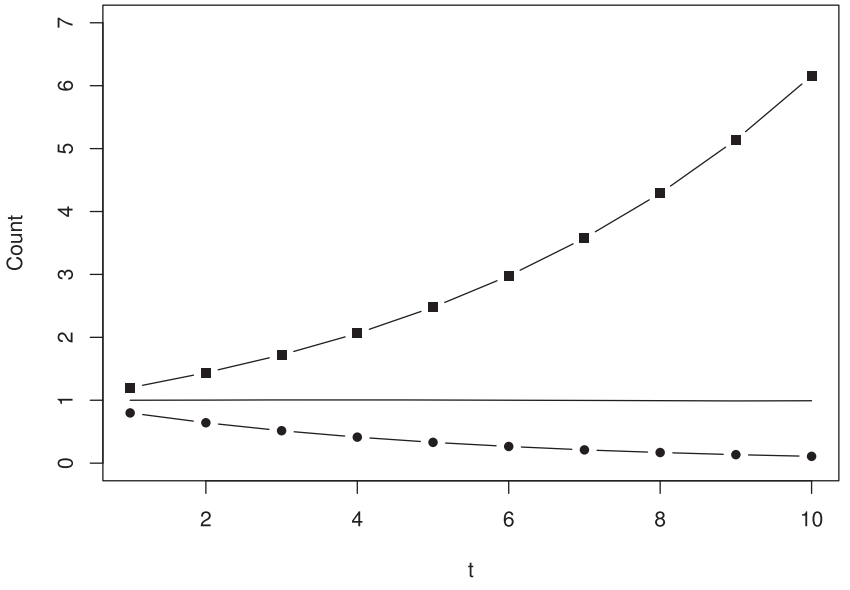

Figure 1. The graphic shows exponential increasing (line with filled square), decreasing (line with filled circle) and population stability (line) for the process $X(t)$. The results are for $p = 2/3$ for supercritical, $p = 1/2$ for critical and $p = 1/3$ for subcritical processes. They are averaged from simulations of 10,000 repetitions for 10 steps ($t = 10$).

Table 1. Summarized values of extinction probabilities for all cases of extinction behaviour.

$\sigma(s)$	$A = F(t,0)$	$1-A$	α	$1-\alpha$
$p = 1$	0	1	$1 - e^{-Kt}$	e^{-Kt}
$1/2 < p < 1$	$\frac{q(1-e^{-mt})}{1-qe^{-mt}}$	$\frac{1-q}{1-qe^{-mt}}$	$\frac{1-e^{-mt}}{1-qe^{-mt}}$	$\frac{(1-q)e^{-mt}}{1-qe^{-mt}}$
$p = 1/2$	$\frac{Kt}{2+Kt}$	$\frac{2}{2+Kt}$	$\frac{Kt}{2+Kt}$	$\frac{2}{2+Kt}$
$0 < p < 1/2$	$\frac{(1-p)(1-e^{mt})}{(1-p)-pe^{mt}}$	$\frac{(1-2p)e^{mt}}{(1-p)-pe^{mt}}$	$\frac{p(1-e^{mt})}{(1-p)-pe^{mt}}$	$\frac{(1-2p)}{(1-p)-pe^{mt}}$

3. Critical birth–death process with random initial conditions

The independence of particle evolution allows us to study the influence of a random initial condition X_0 on the behaviour of the extinction probability. Suppose that the random variable X_0 does not depend on the branching mechanism. Thus a sequence of $X_i(t), i = 1, 2, \ldots$, independent identically distributed linear B–D processes starting with one particle, is considered as the evolution of every one particle entered in the domain of branching at the initial time $t = 0$. The aggregation of independent $X_i(t)$ particles defines a new process $Y(t)$ starting with X_0 random number of particles,

$$Y(t) = \sum_{i=1}^{X_0} X_i(t),\ t > 0, \quad Y(0) = X_0.$$

Let the p.g.f. of initial condition be denoted by $U_0(s) = E[s^{X_0}], U_0(1) = 1, |s| \leq 1$. Then, due to the independence, the p.g.f. of $Y(t)$ is defined by

$$U(t,s) := E[s^{Y(t)} \mid Y(0) = X_0] = U_0(F(t,s)), \quad |s| \leq 1,$$

and satisfies only the following forward Chapman–Kolmogorov equation:

$$\frac{\partial}{\partial t}\left(U(t,s)\right) = \frac{K}{2}(s-1)^2 \frac{\partial}{\partial s}\left(U(t,s)\right),$$

with an initial condition of $U(0,s) = U_0(s)$. The ultimate extinction probability of the new process $Y(t)$ is always equal to 1 because the p.g.f. $U_0(s)$ is continuous at the point $s = 1$, namely,

$$\lim_{t\to\infty} P(Y(t) = 0) = U_0\left(\lim_{t\to\infty} F(t,0)\right) = U_0(1) = 1.$$

For the same reason, the resulting expectation of available particles for any finite time moment $t > 0$ is equal to the mean of the initial condition, $E[Y(t)] = E[X_0]$.

To describe the flux of particles arriving in the domain of branching, a radius R is introduced as a space parameter. In this way, two different options for the location of the initial particles are enabled – either located in one 'point' or dispersed over the radius. The dispersion is described by either simple or marked point processes. There are numerous physical phenomena that can be modelled as a response to the points of a marked point process [see 22, Chapter 4, page 175]. The simple point process is defined by homogeneous Poisson distribution. The marked point process is defined by the compound Poisson distributions such as Negative-Binomial and Pólya–Aeppli ones.

The initial condition strongly influences the ultimate extinction probability q in the supercritical case [see 19]. In the critical case, the ultimate extinction probability is equal to 1 independently of the initial condition. But, there is a relation between the initial condition and the rate of convergence to extinction in a critical branching process. The study of this influence takes a large part of the following sections.

3.1. Geometric distributed initial condition

The first option to construct a random initial sample X_0 is defined by the shifted geometric distribution with probability mass function

$$P(X_0 = k) = (1-\varrho)\varrho^{k-1}, \quad k = 1, 2, \ldots, \ 0 < \varrho < 1. \tag{7}$$

It follows directly from the definition that the p.g.f. of this initial condition is

$$U_0(s) = E[s^{X_0}] = \frac{(1-\varrho)s}{1-\varrho s}, \quad E[X_0] = E[Y(t)] = \frac{1}{1-\varrho}.$$

To find the p.g.f. of process $Y(t)$, the following useful expression is easily yielded directly from Equations (5) and (6):

$$1 - \varrho F(t,s) = \frac{s[Kt(1-\varrho) + 2\varrho] - [2 + Kt(1-\varrho)]}{sKt - (Kt+2)}. \tag{8}$$

Then, using it in expression $U(t,s) = (1-\varrho)F(t,s)/(1-\varrho F(t,s))$ allows the explicit presentation of p.g.f to be obtained, i.e.

$$U(t,s) = \frac{(1-\varrho)[s(Kt-2)-Kt]}{s[Kt(1-\varrho)+2\varrho]-[2+Kt(1-\varrho)]}. \tag{9}$$

This p.g.f. $U(t,s)$ can also be presented in the form showing the geometric distribution of $Y(t)$ at the fixed time $t>0$, namely,

$$U(t,s) = B(t) + (1-B(t))\frac{(1-\beta(t))s}{1-\beta(t)s}, \tag{10}$$

where

$$B(t) = \frac{(1-\varrho)Kt}{2+Kt(1-\varrho)} = U(t,0), \quad \beta(t) = \frac{2\varrho+Kt(1-\varrho)}{2+Kt(1-\varrho)}. \tag{11}$$

Using the last two results, Equations (9) and (10), gives the probability of extinction of process $Y(t)$ by the time $t<\infty$

$$U(t,0) = B(t) = \frac{Kt}{\frac{2}{1-\varrho}+Kt} < \frac{Kt}{2+Kt} = A(t) = F(t,0) < 1.$$

Obviously, the extinction probability decreases by the time $t>0$ when $P(X_0=0)=0$ in a random initial condition.

When the initial condition $\overline{X_0}$ is defined by non-shifted geometric distribution $Ge(\varrho)$, its p.g.f. is $\overline{U}_0(s) = (1-\varrho)/(1-\varrho s), 0<\varrho<1$. Hence, the random number of particles $\overline{Y}(t) = \sum_{i=1}^{\overline{X_0}} X_i(t)$ for any fixed time $t>0$ has a zero-modified geometric distribution with p.g.f. $\overline{U}(t,s)$, represented as follows:

$$\overline{U}(t,s) = C(t) + (1-C(t))\frac{(1-\beta(t))s}{1-\beta(t)s}, \quad \overline{U}(t,0) = C(t) = \frac{B(t)}{A(t)} > B(t),\ t>0, \tag{12}$$

where the parameters $A(t)$, $B(t)$ and $\beta(t)$ are defined by Equations (6) and (11). The parameter $\beta = \beta(t)$ remains the same as for the case of shifted geometric distribution.

It is important to note that the branching process does not start with positive probability $P(X_0=0) = 1-\varrho > 0$ when the initial flux is distributed with non-shifted geometric distribution. This situation implies the inequality $C(t) > B(t)$. Moreover, it is possible to happen either $C(t) > A(t)$ or $C(t) < A(t)$ due to the values of the parameters ϱ and t. Namely, if $\varrho \le 1/2$, i.e. for $P(X_0=0) > 1/2$, the inequality

$$C(t) = \frac{(1-\varrho)(2+Kt)}{2+(1-\varrho)Kt} > A(t) = \frac{Kt}{2+Kt}$$

is valid for all $t>0$. This is equivalent to the following inequality $4(1-\varrho) > 2Kt(2\varrho-1)$.

3.2. Initial condition over the radius of the flux of particles

The usage of geometric distribution enables the construction of random initial samples from binary trials in simulations. To extend this functionality, we consider the dispersion

Table 2. Extinction probabilities in dependence of radius.

	Initial distribution		
	NB[a]	Po	PA
$P(X_0 = 0)$	$(1-\varrho)^R = e^{(\log(1-\varrho))R}$	$e^{-\theta R}$	$e^{-\theta R}$
$P(Y_t = 0)$	$\left(\frac{(1-\varrho)(2+Kt)}{2+(1-\varrho)Kt}\right)^R$	$\exp\left\{\frac{-2\theta R}{2+Kt}\right\}$	$\exp\left\{-\frac{2\theta R}{2+Kt(1-\varrho)}\right\}$

[a]Note that $\theta = -\log(1-\varrho)$.

over a radius of the initial flux entering into the domain of branching. The p.g.f. of the initial condition and the total number of particles alive at the time $t > 0$ are denoted as follows:

$$V_0(R,s) = E[s^{X_0}], \quad V(R,t,s) = E[s^{Z(t)}], \quad Z(t) = \sum_{k=1}^{X_0} X_k(t).$$

The extinction probability is studied by the value of the p.g.f. $V(R,t,s)$ at the point $s = 0$, namely, $V(R,t,0) = P(Z(t) = 0), t > 0$. For different initial conditions, the corresponding extinction probabilities are summarised in Table 2, giving the opportunity to compare them. The first selected distribution for X_0 is the homogeneous Poisson distribution $Po(R,\theta)$ with intensity parameter θ. Another used one is the Negative-Binomial $NB(R,\varrho)$ distribution. In this case, the jumps altitude is defined by the logarithmic series distribution with parameter ϱ and p.g.f. $\log(1-\varrho s)/\log(1-\varrho)$. The intensity parameter is $\theta = -\log(1-\varrho) > 0$. Obviously, the $NB(R,\varrho)$ distribution is reduced to the non-shifted geometric distribution $Ge(\varrho)$ when $R = 1$. The Pólya-Aeppli probability distribution $PA(R,\theta,\varrho)$ is another alternative for X_0. It is a compound Poisson distribution with intensity θ and jumps altitude defined by the shifted geometric distribution in Equation (7). The Pólya-Aeppli probability reduces to the homogeneous Poisson when $\varrho = 0$.

The linear birth–death processes initiated from selected initial conditions yield the following results for p.g.f. $V(R,t,s)$:

(1) Let X_0 be defined by the p.g.f. $V_0(R,s) = \exp\{-\theta R(1-s)\}$ of homogeneous Poisson distribution. Using Equation (5) it is easy to prove that the p.g.f. $V(R,t,s) = E[s^{Z(t)}]$ is equal to

$$V(R,t,s) = \exp\{-\theta R(1-F(t,s))\} = \exp\left\{-\Theta R\left(\frac{1-s}{1-\Upsilon s}\right)\right\}, \tag{13}$$

where the parameters depend on time $t > 0$ as follows:

$$\Theta = \Theta(t) = \frac{2\theta}{2+Kt}, \quad \Upsilon = \Upsilon(t) = \frac{Kt}{2+Kt}. \tag{14}$$

The obtained result in Equation (13) is exactly the p.g.f. of the Pólya–Aeppli probability distribution for fixed time $t > 0$.

(2) Let X_0 be defined by the probability mass function of $NB(R, \varrho)$ distribution:

$$P(X_0 = k) = \frac{\varrho^k (1-\varrho)^R}{k!} \frac{(k+R-1)!}{(R-1)!}, \quad k = 0, 1, \ldots, \ 0 < \varrho < 1.$$

Then the p.g.f. of initial condition is given by

$$V_0(R, s) = \left(\frac{1-\varrho}{1-\varrho s}\right)^R = \exp\left\{-\theta R\left(1 - \frac{-\log(1-\varrho s)}{\theta}\right)\right\}, \quad \theta = -\log(1-\varrho).$$

The expression for p.g.f. $V(R, t, s) = (\overline{U}(t, s))^R$ follows directly from Equation (12) and it is equal to

$$V(R, t, s) = \left(\frac{(1-\varrho)(2+Kt)}{2+(1-\varrho)Kt} + \frac{2\varrho}{2+(1-\varrho)Kt}\frac{(1-\beta)s}{1-\beta s}\right)^R, \tag{15}$$

where $\beta = \beta(t) = (2\varrho + Kt(1-\varrho))/(2 + Kt(1-\varrho))$. The value $V(R, t, 0)$ is shown in Table 2.

(3) Let X_0 be defined by the probability mass function of the Pólya-Aeppli distribution, where $P(X_0 = 0) = e^{-\theta R}$ and

$$P(X_0 = k) = e^{-\theta R} \sum_{j=1}^{k} \binom{k-1}{j-1} \varrho^{k-j} \frac{(\theta R)^j (1-\varrho)^j}{j!}, \quad k = 1, 2, \ldots.$$

Then, the p.g.f. of the initial condition $V_0(R, s) = \exp\{-\theta R((1-s)/(1-\varrho s))\}$. Replacing the expressions $1 - F(t, s)$ and $1 - \varrho F(t, s)$ from Equations (5) and (8) yields

$$V(R, t, s) = \exp\left\{-\theta R \frac{1-F(t,s)}{1-\varrho F(t,s)}\right\} = \exp\left\{-\frac{\Theta R(1-s)}{1-\Upsilon s}\right\}, \tag{16}$$

where the parameters depend on time $t > 0$ as follows:

$$\Theta = \Theta(t) = \frac{2\theta}{2+Kt(1-\varrho)}, \quad \Upsilon = \Upsilon(t) = \frac{2\varrho + Kt(1-\varrho)}{2+Kt(1-\varrho)}. \tag{17}$$

The comparison between the parameters Θ and Υ in the Equations (14) and (17) shows the importance of the parameter ϱ. The respective expressions for the extinction probabilities defined by their values $V(R, t, 0)$ are summarised in Table 2.

4. Computational results

The creation of a well-defined and useful stochastic model is not straightforward – there are many risks and difficulties, partly due to the possible errors in development. To avoid similar pitfalls, the verification of agreements between numerical experiment and already known results is crucial. Therefore, the main topics in the following section are the description of the designed numerical experiment for the studied B–D process and its verification with already obtained analytical results. Finally, underlying the importance of the numerical solutions for complicated branching processes, a well-designed numerical solution could be easily applied and compared to already obtained analytical results in [19] for the supercritical case.

4.1. Computational tools

As a generator of numerical results is considered a computational experiment with branching simulator developed for the R statistical computing environment [26]. It is based on independent simulations following the iterative chain of Equation (2), similar to the one proposed for cosmic rays shower shown in [25]. It works as the transition probabilities for birth and death between different steps that are dependent only on the random variable's current state. They are obtained from independent binary trials at every time step. Therefore, this stochastic experiment produces irreducible and aperiodic transitions after every iteration and can be classified as a Markov chain experiment [3]. Hence, its successful implementation can reproduce numerically chain evolution [see 29].

The selected Markov chain (MC) yields a sequence of random variables $X(0), X(t_1) \ldots,$ $X(t_i)$ with time parameter t_i corresponding to the offspring order. In this case, the simulated results reproduce the desired model with the approximated solution of Equation (5) equal to

$$F(t,s) = s + tf(s) + o(t), \quad t \to 0,$$

with $f(s) = K(1-s)^2/2$. The remainder part $o(t)$ converge to 0 for small t after a long sequence of steps, i.e. for $\Delta = t_{i+1} - t_i, i = 1, 2, \ldots,$ we have

$$\lim_{\Delta \to 0} \frac{F(\Delta, s) - s}{\Delta} = f(s).$$

Thus these simulated results converge to the real one with the extension of the number of steps and repetitions. Finally, it is worth to remark that in case of ordering by heirs number, the daughter particles always arrive in pairs. However, when the process is rearranged with the inclusion of different random lifetime, the pairing breaks according to process modification.

The initial fluxes of Geometric $Ge(\varrho)$, Negative-Binomial $NB(R, \varrho)$ and Poisson $Po(R, \theta)$ distributions are generated using the standard functions available in the R statistical environment. But the additional library named *polyaAeppli* is required for generation of a Pólya–Aeppli distributed population $PA(R, \theta, \varrho)$ [see 7]. The results for every test are registered after 10,000 number of experiment repetitions. Note that the parameter of the intensity of branching (killing rate) K is fixed equal to 1. This simplification is intentional to avoid useless consumption of computational time because K is a scalar constant.

The obtained results from every experiment are structured and therefore they can be easily aggregated by different parameters over all available data sets. The most valuable ones for model description are the probability for extinction and the particle number distribution at every step of experiment $t > 0$. However, their expected distributions usually may not relate to a well-known probabilistic distribution or to be related to any tailed, as obtained Pólya–Aeppli distribution $PA(R, \theta, \varrho)$ in Equation (13). Due to these obstacles, the measure of agreement between distributions is yielded from *k-sample Anderson–Darling (AD)* tests [27]. It is available in R statistical computing environment after installation of the additional *kSamples* library [28].

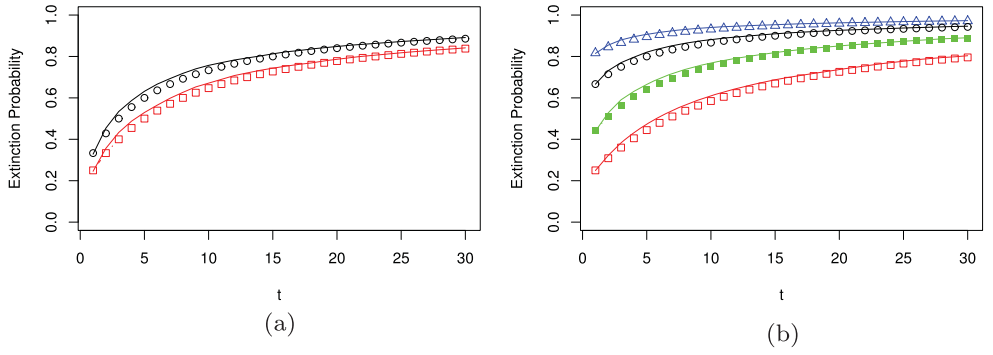

Figure 2. Results for linear birth–death processes with shifted geometric (Figure 2(a)) and Negative-Binomial (Figure 2(b)) distributed initial conditions. Data acquired from experiments are shown with lines. The analytical results of *shifted Ge*(1/2) and *shifted Ge*(1/3) are shown with circles and squares respectively. The predicted results of Negative Binomial experiments are shown with triangles for $NB(1/2, 1/2)$, circles for $NB(1, 1/2)$, filled squares for $NB(2, 1/2)$ and squares for $NB(2, 1/3)$. (a) Extinction probabilities of process with initial shifted geometric distribution. (b) Extinction probabilities of process with initial Negative-Binomial distribution.

4.2. Experimental results

Initially, the experiments are run separately for the B–D process with $Ge(\varrho)$, $NB(R, \varrho)$, $Po(R, \theta)$ and $PA(R, \theta, \varrho)$ distributed initial particle flux. By definitions, the selected four distributions are inter-related. Using this property, the parameters are specially considered to be inter-compatible between different experiments. At first, for example, the relations between processes with $Ge(\varrho)$ and $NB(R, \varrho)$ distributed initial conditions are tested for equivalence between $NB(R, \varrho)$ distribution with $R = 1$ and *non-shifted* $Ge(\varrho)$ when the parameter ϱ is the same. Later, the equivalence by radius parameter R of extinction probabilities of B–D processes with $NB(R, \varrho)$ and $Ge(\varrho)$ distributed initial conditions is confirmed after directly applying Equation (15). As expected, the results from *k-sample AD* tests between simulated samples clearly confirm equivalences for all of them with *p*-values above 0.99. The last option to have compatible results is to select equal evolution parameters in the interval of $t \in (0, 30]$ for all tests.

Thus the values of ϱ of the *shifted* $Ge(\varrho)$ and $NB(R, \varrho)$ distributions are selected respectively $\{1/3, 1/2\}$. The additional radius parameter $[0, R)$ for $NB(R, \varrho)$ distributed initial conditions is selected to take four options equal to $\{1/2; 1; 2; 5\}$. To keep inter-compatibility clear, there is a complete set of experiments with all possible values of $B(t) = U(t, 0)$ but all with $\varrho = 1/2$. A similar work-flow is selected for testing Poisson distributed initial flux. The selected test values of the radius R for $NB(R, \varrho)$ are combined with the newly introduced values of $\theta = \{1; 2\}$. The analytically computed extinction values are directly obtained from formulas shown in Table 2 for all simulated $t > 0$. The agreement between them and the experiment is shown graphically in Figures 2 and 3. The computed *p*-values from the *k-sample AD* tests are shown in Table 3.

The results show a good agreement between the analytical estimates and the simulated extinction probability values. In addition, the increases of *p*-values with a growing number of steps $t_i > 0$ are observed for most of the tests. For instance, the *p*-value measure of goodness-of-fit for B–D process initiated from $NB(2, 1/2)$ distributed initial flux grows

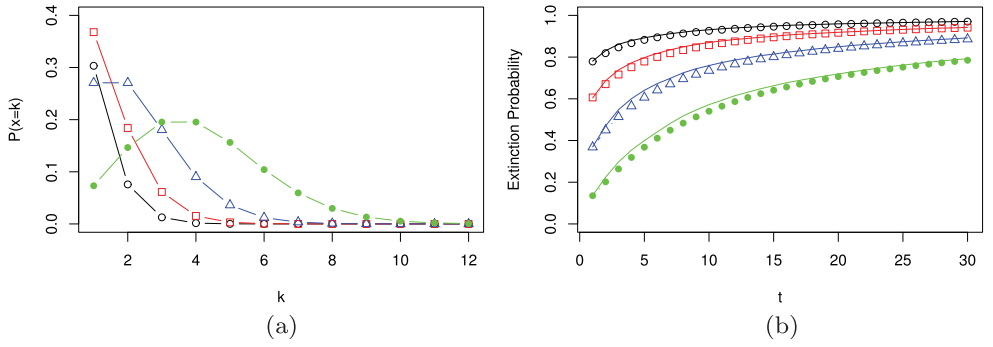

Figure 3. Results for linear birth–death process with Poisson initial conditions. The distributions of the selected initial conditions are shown in Figure 3(a). The extinction probabilities for analytical and experimental solutions are shown in Figure 3(b). The different experiments and their initial conditions are shown with different figures: $Po(1/2, 1)$ with circles, $Po(1, 1)$ with squares, $Po(2, 1)$ with triangle point-up and $Po(2, 2)$ with filled circles. (a) The initial conditions. (b) Extinction probabilities.

Table 3. Comparison between $V(R, t, 0)$ obtained from experiments and analytical predictions for linear B–D processes with initial conditions distributed with *shifted Ge*(ρ), $NB(R, \rho)$ and $Po(R, \theta)$.

				p-values							*p*-values		
Distribution	θ	R	ϱ	$t = 10$	$t = 20$	$t = 30$	Distribution	θ	R	ϱ	$t = 10$	$t = 20$	$t = 30$
shifted Ge	–	–	1/2	0.866	0.933	0.975	*NB*	–	2	1/3	0.866	0.933	0.975
shifted Ge	–	–	1/3	0.914	0.961	0.999	*Po*	1	1/2	–	0.988	0.949	0.999
NB	–	1/2	1/2	0.729	0.601	0.754	*Po*	1	1	–	0.82	0.984	0.999
NB	–	1	1/2	0.776	0.696	0.822	*Po*	1	2	–	0.82	0.923	0.971
NB	–	2	1/2	0.866	0.99	0.999	*Po*	1	5	–	0.866	0.933	0.975
NB	–	5	1/2	0.82	0.923	0.971	*Po*	2	2	–	0.914	0.942	0.978

from 0.866 to 0.999. Actually, the results show that experiments of only 10 steps are enough to produce close to expected results. Moreover, the p-values of fit for most of the cases easily grows above 95% for $t > 25$. This implies a complete convergence between the theory and experiment with $t \to \infty$.

However, there are a number of tests that show weak divergence in an agreement between experiment and theory at steps between 10 and 30. For them, the *k-sample AD* test's p-values are worse in comparison to the earlier stages but still high enough to confirm the agreement after about 15–20 steps. An example is the experiment of $NB(1, 1/2)$. The explanation is related to the importance of the initial condition in the process of selection. For the critical case, it is known that the average number of particles at every $t > 0$ varies over the initial number. However, the number of died families (with all heirs death) is growing during the process development. This means that the average number at every step $t > 0$ is compensated by an explosion of the survived families' heirs, i.e. *the winner takes all*. It is demonstrated very clearly in population distribution after 30 step B–D process with Poisson distributed initial conditions, shown in Figure 4.

Hence, the selection process stretches particle distribution differently and thus making the initial state of linear B–D processes very important. When there is a high chance of zero occurrences in the initial flux, the process $Y(t)$ is less prone to explode and the small number of survived heirs variate highly. The result is a slower and with a non-constant

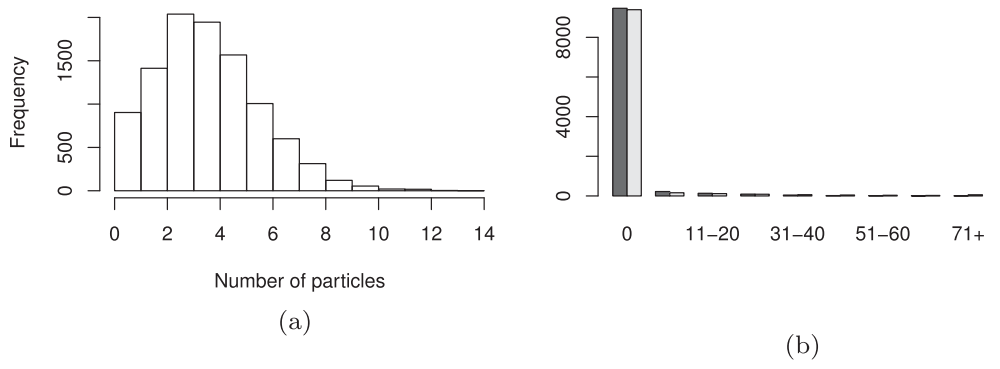

Figure 4. Histograms of Poisson distributed particle population before and after experiment. (a) Poisson distributed particles in the initial moment. (b) Particles distribution (dark) and expected Pólya–Aeppli distribution after 30 steps.

Table 4. Results from goodness-of-fit tests for extinctions of Pólya–Aeppli distributed initial fluxes.

Distribution	$R\theta$	ϱ	*k-sample AD* test *p*-value	Distribution	$R\theta$	ϱ	AD test *p*-value
$PA(R,\theta,\varrho)$	1	1/2	0.504	$PA(R,\theta,\varrho)$	4	1/2	0.985
$PA(R,\theta,\varrho)$	1	1/3	0.5653	$PA(R,\theta,\varrho)$	4	1/3	0.9866

improvement of agreements between experiment and expected values at intermediate steps, giving lower and varied *p*-values for long period whenever the initial conditions are similar to the example of $NB(1,1/2)$ distribution. Conversely, when the number of zero events in the initial flux are very low, the B–D processes extinct slowly and without serious fluctuations in the middle steps.

Finally, the experiments with Pólya–Aeppli distributed initial flux are intentionally considered to combine properties of the $Po(R,\theta)$ and $NB(R,\varrho)$ distributions. For this reason, the used distribution parameters are a combination of already selected values in previous experiments. Moreover, it is easy to notice from Table 2 that for $\varrho = 0$ the extinction probabilities are equal to these of Poisson initiated processes. Thus $R\theta$ is selected to be optional between $\{1,4\}$ in combinations with $\rho = \{1/3,1/2\}$. This enables the introduction of more complex distributions for initial particle flux, such as shown $PA(R,\theta,\varrho)$ distributions in Figure 5(a). For them, the experimental data show that the properties are similar to those already observed for Poisson and Negative-Binomial, but in combined effect dependent on ϱ due to differences between parameters Θ and Υ in the Equations (14) and (17). The numerical results of agreement for $t = 30$ between survived particles in experiment and analytically computed values from Equation (16) are shown in Table 4 and Figure 5(b).

5. Extending complexity

To create more useful and real-life applications, the designed experiment has to be expanded to a more complex B–D process. The selection of more complicate initial conditions is one of the options. An interesting choice for this is the implementation of Pólya urn processes. They are part of developing theory with many different applications, mainly in theoretical physics, such as [11].

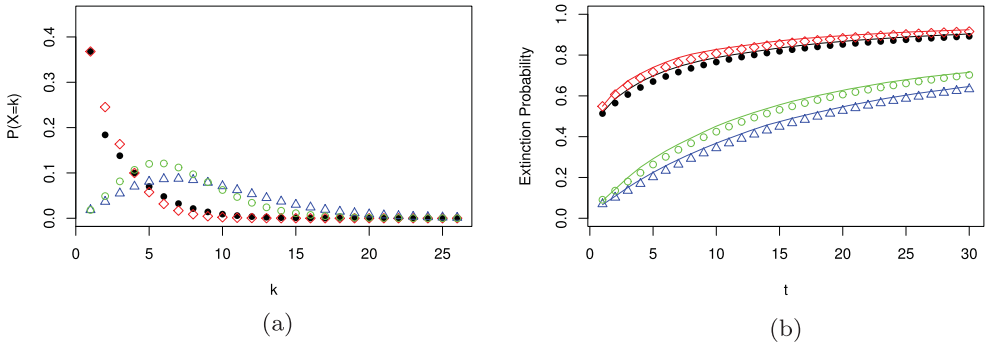

Figure 5. Results for linear birth–death process with Pólya–Aeppli initial conditions. The distributions of the selected initial conditions are shown in Figure 5(a). The extinction probabilities for analytical and experimental solutions are shown in Figure 5(b). The different experiments and their initial conditions are shown with different figures: $PA(1, 1, 1/2)$ with filled circles, $PA(1, 1, 1/3)$ with diamonds, $PA(2, 2, 1/2)$ with triangle point-up and $PA(2, 2, 1/3)$ with empty circles. (a) The initial conditions. (b) Extinction probabilities.

The selected initial state is designed to be generated with a multi-state Pólya urn processes using Pólya urn experiment. It is self-reinforcing processes that resemble the situation of the *the winner takes all* phenomenon and it is close to a beta-binomial distribution, Dirichlet processes and applications in genetics. The process, in general, is assumed for an urn with A_0 number of white and black balls in an initial proportion equal to $\sigma = (number - white)/(number - black)$ and a deterministic replacement matrix M. The process proceeds when the balls are drawn consecutively. If a black one is drawn, a black and b white number of balls are returned to the urn in addition to the already selected black one. Similarly, in case of a drawn white ball, c black and $d + 1$ white number of balls are returned. The process could be generalized as

$$M = \begin{bmatrix} a & b \\ c & d \end{bmatrix}; \quad a, b \in N_0 \cup \{-1\}; \quad b, c \in N_0 := \{0, 1, 2, \ldots\},$$

where $a + b = c + d \geq 1$. There are many models derived from similar urn process. For example, a Moran process is assumed in connection with branching processes in genetics [see 2] and two colours Pólya urn process with possible growth (or shrinkage) of the population, [see 8,15].

However, in this section, only a simplified Pólya urn experiment proposed in [11] is considered as a generator for random initial conditions. In every step, a single ball is drawn with a binary trial. When the colour is known, δ-number additional balls in the same colours are returned to its place in the urn. When the drawn ball is black, $\delta = a$, or conversely to $\delta = d$ in case of a white ball. The other values of matrix M are zeroes, i.e. $b = c = 0$. The random initial condition of our process $Y(t)$ is obtained after numbers of random consecutive urn draws. The reinforcement parameter is introduced with $\gamma := \delta/A_0$ and N is the number of samples drawn from the urn. Then, when $\gamma = \delta/A_0 \to 0$ for $N \to \infty$, the process behaves similarly to binomial, in spite of the large values of δ [11]. For reproducing different reinforcements, the population is generated after a small number of $N = 10$ trials. The number of fractions of γ is produced from combinations of different initial particle

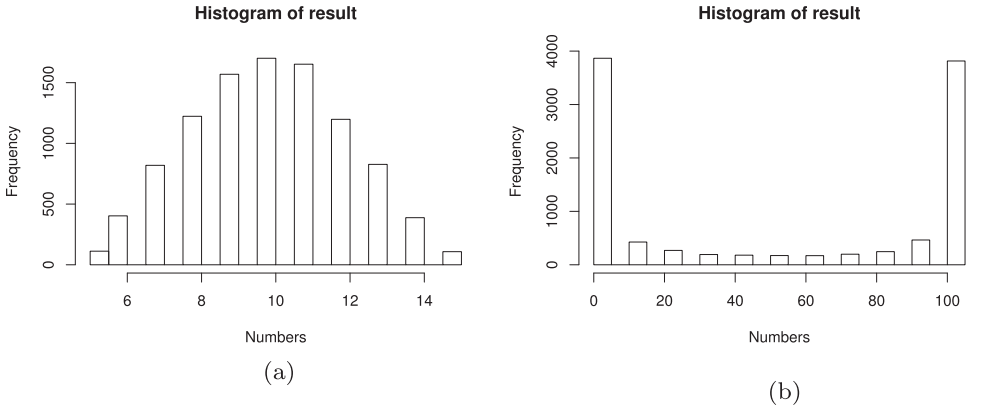

Figure 6. Distribution of Pólya urn after $N = 10$ trials of equally distributed ($\sigma = 1$) balls after 10000 repetitions. The differences are due to values of *delta* and A_0. (a) 'Almost' binomial trials with $\delta = 1$ and $A_0 = 10$. (b) *The winner takes all* situation with $\delta = 10$ and $A_0 = 2$.

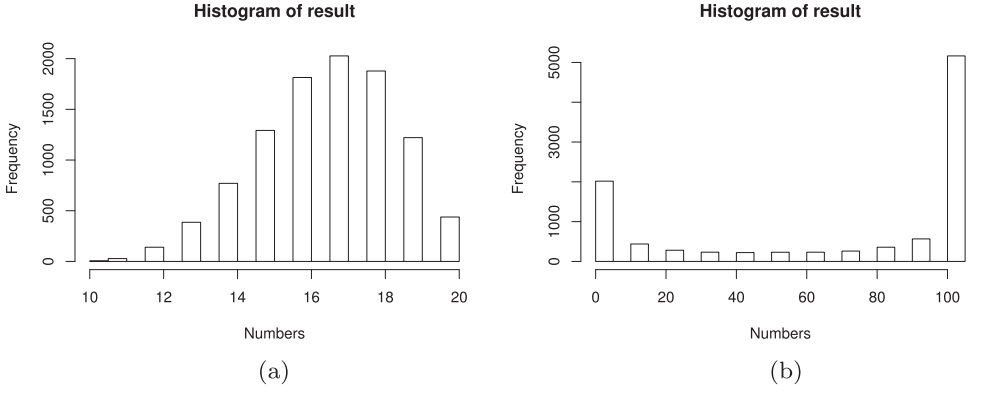

Figure 7. Distribution of Pólya urn after $N = 10$ trials with asymmetric distributed ($\sigma = 2$) balls after 10000 repetitions. The differences are due to values of *delta* and A_0. (a) 'Almost' binomial trials with $\delta = 1$ and $A_0 = 10$. (b) *The winner takes all* situation with $\delta = 10$ and $A_0 = 2$.

numbers $A_0 = \{2; 10\}$ and fractions $\sigma = \{1; 2\}$. Some of the generated results are shown in Figures 6 and 7.

The experimental results are the only available source of information for the process. There are two main conclusions that could be yielded from experiments. The first one is that after a very long run, σ parameter of urn experiment does not impact the rate of extinction, but only the initial distribution. The important parameter of initial condition is δ. The impact of different δ is clearly demonstrated in Figure 8(a) with resulting clusterization of simulated extinction probabilities. Secondly, due to the process of selection, the distribution of daughter particles is stretched similarly to the previous models with Poisson and Pólya-Aeppli distributed initial flux. Moreover, the resulting distribution is easily proved as Pólya-Aeppli when X_0 is obtained from a *winner takes all* experiment. It is a direct result from the convergence of Binomial distribution to Poisson when the number of trials is sufficiently bigger than the mean number of successes. In our case, the expected parameters

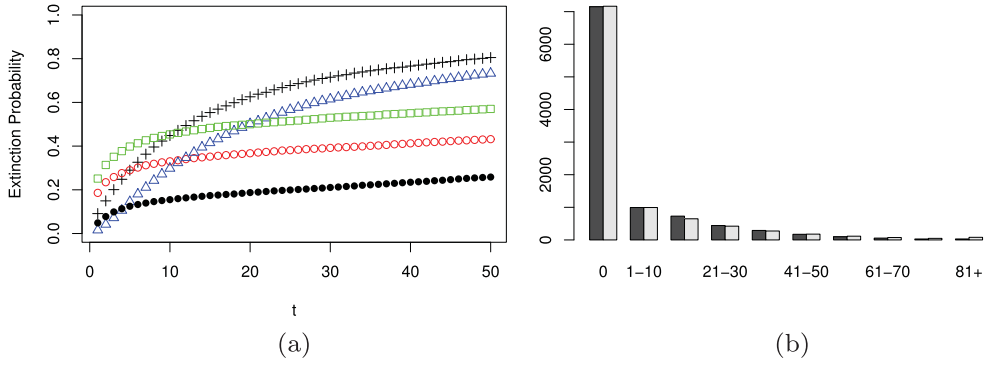

Figure 8. Graphics show different extinctions of process with initial flux distributed by 10 consecutive Polya urn draws for $t \in (1:50]$ (Figure 8(a)). The initial number of particles is $A_0 = 2$. The agreement with Pólya–Aeppli distributions is demonstrated in Figure 8(b). (a) Different figures are used for processes initiated with: pluses for $\sigma = 1$ and $\delta = 1$; circles for $\sigma = 1$ and $\delta = 10$; triangles for $\sigma = 2$ and $\delta = 1$; filled circles for $\sigma = 2$ and $\delta = 10$; squares for $\sigma = 1/2$ and $\delta = 10$. (b) The outcome of experiment with initial conditions after Polya urn game with $\sigma = 1$ and $\delta = 1$ (in dark) and $PA(R\theta = 1/3, 19/20)$ (white colour).

of distribution $Y(t)$ at any moment $t > 0$ could be computed from the experimental data with automatic procedure for *k-sample AD* test. The most simple procedure to do it is to generate as much as possible hypothesises by combinations of a large set of possible parameters and eliminate the options with low p-values of *k-sample AD* test. As an example, a fit with $PA(R\theta = 1/3, 19/20)$ is confirmed as good for linear B-D experiment after $t = 30$ steps of branching. The initial flux X_0 is generated with Pólya urn game with $\sigma = 1$ and $\delta = 1$ (Figure 8(b)). The hypothesis is tested and confirmed with p-values above 0.9 from *k-Sample AD tests*.

6. Conclusion

The demonstrated results contribute mainly to applications of branching processes. First, they are related to applications with outcome produced from branching processes where the initial conditions are important. Second, with the obtained results is demonstrated a possible method for numerical solution when the analytical estimates are infeasible. The proposed usage of computational experiments is proved and well fitted to the theory. This makes any partial or full implementation of similar methods possible as a part of any other large scale Monte Carlo experiments. The expected solutions also may include or extend any random distributed initial condition in consideration of the available experiment. Finally, the obtained results may be useful as a reference for further statistical analysis of the output from similar processes.

A similar simulator may be used either as a standalone application in any particular study or as a part of more complex systems. The complexities could be due to any natural processes that are even in particularly related to branching models. For example, any further consideration of immigrations or censoring could extend applicability to many natural processes. Other possible real-life applications where similar approach can be implemented

are models with non-homogeneous time intervals between birth and death events. Moreover, similar methods for solving very complex natural systems could be implemented technically easily to larger class of Markov branching processes due to quickly expanding computational power.

Disclosure statement

No potential conflict of interest was reported by the author(s).

Funding

This research is partially supported by the Bulgarian National Science Fund, grant No KP-06-H22/3.

ORCID

A. Tchorbadjieff http://orcid.org/0000-0001-9322-262X

References

[1] S. Agostinelli, J. Allison, K. Amako, J. Apostolakis, H. Araujo, P. Arce, M. Asai, D. Axen, S. Banerjee, G. Barrand, F. Behner, L. Bellagamba, J. Boudreau, L. Broglia, A. Brunengo, H. Burkhardt, S. Chauvie, J. Chuma, R. Chytracek, G. Cooperman, G. Cosmo, P. Degtyarenko, A. Dell'Acqua, G. Depaola, D. Dietrich, R. Enami, A. Feliciello, C. Ferguson, H. Fesefeldt, G. Folger, F. Foppiano, A. Forti, S. Garelli, S. Giani, R. Giannitrapani, D. Gibin, J.J. Gómez Cadenas, I. González, G. Gracia Abril, G. Greeniaus, W. Greiner, V. Grichine, A. Grossheim, S. Guatelli, P. Gumplinger, R. Hamatsu, K. Hashimoto, H. Hasui, A. Heikkinen, A. Howard, V. Ivanchenko, A. Johnson, F.W. Jones, J. Kallenbach, N. Kanaya, M. Kawabata, Y. Kawabata, M. Kawaguti, S. Kelner, P. Kent, A. Kimura, T. Kodama, R. Kokoulin, M. Kossov, H. Kurashige, E. Lamanna, T. Lampén, V. Lara, V. Lefebure, F. Lei, M. Liendl, W. Lockman, F. Longo, S. Magni, M. Maire, E. Medernach, K. Minamimoto, P. Mora de Freitas, Y. Morita, K. Murakami, M. Nagamatu, R. Nartallo, P. Nieminen, T. Nishimura, K. Ohtsubo, M. Okamura, S. O'Neale, Y. Oohata, K. Paech, J. Perl, A. Pfeiffer, M.G. Pia, F. Ranjard, A. Rybin, S. Sadilov, E. Di Salvo, G. Santin, T. Sasaki, N. Savvas, Y. Sawada, S. Scherer, S. Sei, V. Sirotenko, D. Smith, N. Starkov, H. Stoecker, J. Sulkimo, M. Takahata, S. Tanaka, E. Tcherniaev, E. Safai Tehrani, M. Tropeano, P. Truscott, H. Uno, L. Urban, P. Urban, M. Verderi, A. Walkden, W. Wander, H. Weber, J.P. Wellisch, T. Wenaus, D.C. Williams, D. Wright, T. Yamada, H. Yoshida, and D. Zschiesche, *GEANT4-a simulation toolkit*, Nucl. Instrum. Methods Phys. Res. A 506 (2003), pp. 250–303.

[2] P. Altrock, L.L. Liu, and F. Michor, *The mathematics of cancer: integrating quantitative models*, Nat. Rev. Cancer 15 (2015), pp. 730–745.

[3] Ch. Andrieu, N. de Freitas, A. Doucet, and M.I. Jordan, *An introduction to MCMC for machine learning*, Mach. Learn. 50 (2003), pp. 5–43.

[4] K. Athreya and P. Ney, *Branching Processes*, Springer, New York, 1972.

[5] E. Baake and A. Wakolbinger, *Feller's contributions in mathematical biology*, in *The Selected Papers of William Feller*, R. L. Schilling, Z. Vondracek, W. A. Woyczynski, eds., Vol. 2, Springer Verlag, Heidelberg, 2015, pp. 25–43.

[6] G. Battistoni, S. Muraro, P.R. Sala, F. Cerutti, A. Ferrari, S. Roesler, A. Fasso, and J. Ranft, *The fluka code: description and benchmarking*, AIP Conference Proceedings, Batavia, IL, USA, Vol. 896, 2006, pp. 31–49. Available at https://aip.scitation.org/toc/apc/896/1.

[7] C. Burden, *polyaAeppli: Implementation of the Polya-Aeppli distribution*, R package version 2.0, 2014. Available at https://CRAN.R-project.org/package = polyaAeppli.

[8] B. Chauvin, N. Pouyanne, and R. Sahnoun, *Limit distributions for large Pólya urns*, Ann. Appl. Probab. 21 (2011), pp. 1–32.

[9] R. Dascaliuc, N. Michalowski, E. Thomann, and E.C. Waymire, *A delayed yule process*, Proc. Amer. Math. Soc. 146 (2018), pp. 1335–1346. doi:10.1090/proc/13905.
[10] M. Elia and G. Taracco, *A note on linear birth-and-death processes*, Mathl. Comput. Modeling 16 (1992), pp. 61–69.
[11] R. Hanel, B. Corominas-Murtra, and S. Thurner, *Understanding frequency distributions of path-dependent processes with non-multinomial maximum entropy approaches*, New. J. Phys. 19 (2017), pp. 033008.
[12] T. Harris, *The Theory of Branching Processes*, Springer, New York, 1963.
[13] D. Heck, J. Knapp, J.N. Capdevielle, G. Schatz, and T. Thouw, *CORSIKA: a Monte Carlo code to simulate extensive air showers*, D-30167 Hannover, Forschungszentrum Karlsruhe GmbH, Karlsruhe (Germany), 1998.
[14] D.G. Kendal, *Branching processes since 1873*, J. London Math. Soc. 41 (1966), pp. 385–406. doi:10.1112/jlms/s1-41.1.385.
[15] M. Knape and R. Neininger, *Plya urns via the contraction method*, Comb. Probab. Comput. 23 (2014), pp. 1148–1186.
[16] G.B. Kristiansen, G.V. Kulikov, and Y.A. Fomin, *Ultrahigh Energy Cosmic Rays*, 1975, (in Russian).
[17] P. Mayster, *Subordinated Markov branching processes and Lévy processes*, Serdica Math. J. 40 (2014), pp. 183–208.
[18] P. Mayster, *Consecutive subordination of Poisson processes and gamma processes*, Compt. Rend. Acad. Bulg. Sci. 71 (2018), pp. 735–742. doi:10.7546/CRABS.2018.06.02.
[19] P. Mayster and A. Tchorbadjieff, *Supercritical Markov branching process with random initial condition*, Compt. Rend. Acad. Bulg. Sci. 72 (2019), pp. 21–28. doi:10.7546/CRABS.2019.01.03.
[20] B.A. Sevasyanov, *Branching processes*, Moskow, Nauka, 1971, (in Russian); B. A. Sewastjanow, *Verzweigungsprozesse*, R. Oldenbourg Verlag, Munich, 1975, (in German).
[21] M. Slavtchova-Bojkova, P. Trayanov, and S. Dimitrov, *Branching processes in continuous time as models of mutations: computational approaches and algorithms*, Comput. Stat. Data. Anal. 113 (2017), pp. 111–124.
[22] D.L. Snyder and M.I. Miller, *Random Point Processes in Time and Space*, 2nd ed., Springer Texts in Electrical Engineering, Springer, New York, 1991. doi:10.1007/978-1-4612-3166-0.
[23] A. Putze, L. Derome, D. Maurin, L. Perroto, and R. Taillet, *A markov chain Monte Carlo technique to sample transport and source parameters of galactic cosmic rays*, Astron. Astrophys. 497 (2009), pp. 991–1007.
[24] S. Tavaré, *The linear birth – death process: an inferential retrospective*, Adv. Appl. Probab. 50 (2018), pp. 253–269. doi:10.1017/apr.2018.84.
[25] A. Tchorbadjieff, *Using branching processes to simulate cosmic rays cascades*, Pliska Stud. Math. 27 (2017), pp. 103–114.
[26] R Foundation for Statistical Computing, *R: A Language and Environment for Statistical Computing*, 2018, Available at https://www.R-project.org/.
[27] F.W. Scholz and M.A. Stephens, *K-Sample Anderson-Darling tests*, J. Am. Stat. Assoc. 82 (1987), pp. 918–924.
[28] F. Scholz and A. Zhu, *kSamples: K-Sample Rank Tests and their Combinations*, R package version 1.2-8, 2018, Available at https://CRAN.R-project.org/package = kSamples.
[29] B. Walsh, *Markov Chain Monte Carlo and Gibbs Sampling*, Lecture Notes for EEB 581, version 26, 2004.
[30] G.U. Yule, *A mathematical theory of evolution, based on the conclusions of Dr. J. C. Willis, F.R.S*, Philos. Trans. R. Soc. B. 213 (1925), pp. 21–87. doi:10.1098/rstb.1925.0002.